

Parton Momentum Distribution at the Moment of Jet-Parton Collisions

Cheuk-Yin Wong*

Physics Division, Oak Ridge National Laboratory, Oak Ridge, TN 37831, U.S.A.

(Dated: November 27, 2018)

We extract the early parton momentum distribution using the STAR Collaboration data of ridge particles associated with a near-side jet in central AuAu collisions at $\sqrt{s_{NN}} = 200$ GeV. The ridge particles are identified as medium partons kicked by the jet near the surface and they carry direct information on the parton momentum distribution at the moment of jet-parton collisions. The extracted parton momentum distribution has a thermal-like transverse momentum distribution but a rapidity plateau structure with a relatively flat rapidity distribution at mid-rapidities with sharp kinematic boundaries at large rapidities that depend on the transverse momentum.

PACS numbers: 25.75.Gz 25.75.Dw

In central high-energy heavy-ion collisions, the state of the parton medium during the early stage of a nucleus-nucleus collision is an important physical quantity. On the one hand, it furnishes information for the investigation of the mechanism of parton production in the early stages of the collision of two heavy nuclei. On the other hand, it provides the initial information for the evolution of the system toward the state of quark-gluon plasma. Not much is known about the early state of the partons from direct experimental measurements.

Recently, the STAR Collaboration observed a $\Delta\phi$ - $\Delta\eta$ correlation of particles associated with a near-side jet in central AuAu collisions at $\sqrt{s_{NN}} = 200$ GeV at RHIC, where $\Delta\phi$ and $\Delta\eta$ are the azimuthal angle and pseudo-rapidity differences relative to a high- p_t trigger particle [1, 2, 3, 4, 5]. The near-side correlations can be decomposed into a “jet” component as fragmentation and radiation products of the near-side jet at $(\Delta\phi, \Delta\eta) \sim (0, 0)$, and a “ridge” component at $\Delta\phi \sim 0$ with a ridge structure in $\Delta\eta$.

While many theoretical models have been proposed [6, 7, 8, 9, 10, 11, 12, 13, 14, 15, 16, 17, 18], a momentum kick model was put forth to describe the ridge phenomenon [11, 12, 13]. The model assumes that a near-side jet occurs near the surface and it kicks medium partons, loses energy along its way, and fragments into the trigger particle and other fragmentation and radiation products in the “jet” component. The kicked medium partons, each of which acquires a momentum kick from the near-side jet, materialize by parton-hadron duality as ridge particles. They carry direct information on the parton momentum distribution at the moment of jet-parton collisions.

We shall extract this parton momentum distribution for central AuAu collisions at $\sqrt{s_{NN}} = 200$ GeV using the STAR data [1, 3, 4]. In a central AuAu collision, jet partons with a distribution $dN_j/d\mathbf{p}_j$ occur near the medium surface. The number of trigger particles reach-

ing the near-side detector with momentum \mathbf{p}_{trig} is

$$N_{\text{trig}} = \int d\mathbf{p}_j \frac{dN_j}{d\mathbf{p}_j} \sum_{N=0}^{N_{\text{max}}} P_N(N) e^{-\zeta N} D(\mathbf{p}_{\text{trig}}; \mathbf{p}_j - \sum_{n=1}^N \mathbf{q}_n), \quad (1)$$

where N is the number of medium partons kicked by the jet, with a maximum N_{max} , and $P_N(N)$ is a geometry-dependent probability distribution of N normalized by $\sum_{N=0}^{N_{\text{max}}} P_N(N) = 1$. The factor $e^{-\zeta}$ describes the inelastic attenuation of the jet for each jet-(medium parton) collision, and $D(\mathbf{p}_a; \mathbf{p}_b)$ is the fragmentation function for fragmenting a \mathbf{p}_a hadron from a \mathbf{p}_b parton. The distribution of the associated kicked partons is therefore

$$\begin{aligned} \frac{dN_{\text{ridge}}^{AA}}{d\mathbf{p}} &= \int d\mathbf{p}_j \frac{dN_j}{d\mathbf{p}_j} \sum_{N=1}^{N_{\text{max}}} P_N(N) e^{-\zeta N} \\ &\times D(\mathbf{p}_{\text{trig}}; \mathbf{p}_j - \sum_{n=1}^N \mathbf{q}_n) \frac{2}{3} \sum_{n=1}^N \frac{dF_n}{d\mathbf{p}}(\mathbf{q}_n), \quad (2) \end{aligned}$$

where $dF_n/d\mathbf{p}$ is the momentum distribution of the n -th kicked medium parton, normalized to $\int d\mathbf{p} dF_n/d\mathbf{p} = 1$, and the factor $(2/3)$ arises since the ridge particle detector accepts only charged particles. The formulation is greatly simplified upon representing $dF_n/d\mathbf{p}$ by the average $dF/d\mathbf{p}$ and taking the different momentum kicks \mathbf{q}_n to be the average \mathbf{q} . We then obtain

$$\frac{1}{N_{\text{trig}}} \frac{dN_{\text{ridge}}^{AA}}{d\mathbf{p}} = \frac{2}{3} \langle N \rangle \frac{dF}{d\mathbf{p}}(\mathbf{q}) = \frac{2}{3} \langle N \rangle \frac{dF}{d\mathbf{p}}(\mathbf{q}), \quad (3)$$

where $\langle N \rangle$ is the average number of kicked partons per trigger particle as determined from Eqs. (1) and (2),

$$\begin{aligned} \langle N \rangle &= \frac{1}{N_{\text{trig}}} \int d\mathbf{p}_j \frac{dN_j}{d\mathbf{p}_j} \sum_{N=0}^{N_{\text{max}}} N P_N(N) e^{-\zeta N} \\ &\times D(\mathbf{p}_{\text{trig}}; \mathbf{p}_j - \sum_{n=1}^N \mathbf{q}_n). \quad (4) \end{aligned}$$

On the other hand, the distribution of the “jet” component of associated fragmentation and radiation products

*Email: wongc@ornl.gov

is given by

$$\frac{dN_{\text{jet}}^{AA}}{d\mathbf{p}} = \int d\mathbf{p}_j \frac{dN_j}{d\mathbf{p}_j} \sum_{N=0}^{N_{\text{max}}} P_N(N) e^{-\zeta N} \times D_2(\mathbf{p}_{\text{trig}}, \mathbf{p}; \mathbf{p}_j - \sum_{n=1}^N \mathbf{q}_n), \quad (5)$$

where $D_2(\mathbf{p}_a, \mathbf{p}_b; \mathbf{p}_c)$ is the double fragmentation function for fragmenting \mathbf{p}_a and \mathbf{p}_b hadrons from a jet parton of momentum \mathbf{p}_c . Fragmentation measurements [3] suggest an approximate scaling relation

$$D_2(\mathbf{p}_{\text{trig}}, \mathbf{p}; \mathbf{p}_c) \approx D(\mathbf{p}_{\text{trig}}; \mathbf{p}_c) D_z(\mathbf{p}; \mathbf{p}_{\text{trig}}), \quad (6)$$

where $D_z(\mathbf{p}; \mathbf{p}_{\text{trig}})$ is approximately the same (within a factor of about 0.6 to 1.2) for dAu and AuAu collisions in $2.5 < p_{t,\text{trig}} < 6$ GeV (Fig. 5b and 5c of [3]). Applying this approximate scaling relation to Eq. (5), the jet component in an AA central collision per trigger is

$$\frac{1}{N_{\text{trig}}} \frac{dN_{\text{jet}}^{AA}}{d\mathbf{p}} \approx D_z(\mathbf{p}; \mathbf{p}_{\text{trig}}) \approx \frac{dN_{\text{jet}}^{pp}}{d\mathbf{p}}. \quad (7)$$

Because of the approximate nature of the above relation, we need to make a quantitative check. In the region where the jet component has a prominent appearance, as in Fig. 1(d) for $2 < p_t < 4$ GeV, the total $dN_{\text{ch}}/N_{\text{trig}} d\Delta\eta$ distribution at $\Delta\eta \sim 0$ has indeed a similar shape as, but a peak magnitude about equal to, the pp near-side jet distribution. Because the total yield is the sum of the jet component and ridge yields and the ridge yield at $\Delta\eta \sim 0$ is non-zero, the near-side jet component in AuAu central collisions per trigger is thus an attenuated pp near-side jet distribution, as expected for production in an interacting medium. If one assumes that fragmentation products lying deeper than an absorption length from the surface are all absorbed, then the average jet fragment transmission factor is $f_J = \int_0^\lambda e^{-x/\lambda} dx / \lambda = 0.632$, which also leads to a reasonable semi-empirical description of the experimental data as indicated below in Figs. 1 and 2. A ridge particle transmission factor f_R can be similarly introduced, but present measurements furnish information only on the product $f_R(N)$. The sum of the distributions (3) and (7), relative to the trigger particle angles, is therefore given more precisely as

$$\left[\frac{1}{N_{\text{trig}}} \frac{dN_{\text{ch}}}{p_t dp_t d\Delta\eta d\Delta\phi} \right]_{\text{total}}^{AA} = \left[f_R \frac{2}{3} \langle N \rangle \frac{dF}{p_t dp_t d\Delta\eta d\Delta\phi} \right]_{\text{ridge}}^{AA} + \left[f_J \frac{dN_{\text{jet}}^{pp}}{p_t dp_t d\Delta\eta d\Delta\phi} \right]_{\text{jet}}^{AA}. \quad (8)$$

In the momentum kick model, the normalized ridge particle momentum distribution $dF/d\mathbf{p}$ at \mathbf{p} is related to the normalized initial parton momentum distribution at a shifted momentum, $\mathbf{p}_i = \mathbf{p} - \mathbf{q}$, and we have [11]

$$\frac{dF}{p_t dp_t d\eta d\phi} = \left[\frac{dF}{p_{ti} dp_{ti} dy_i d\phi_i} \frac{E}{E_i} \right]_{\mathbf{p}_i = \mathbf{p} - \mathbf{q}}$$

$$\times \sqrt{1 - \frac{m^2}{(m^2 + p_{ti}^2) \cosh^2 y}}, \quad (9)$$

where the factor E/E_i insures conservation of particle number and the last factor changes the rapidity to pseudorapidity distribution [19]. Therefore, the ridge particle momentum distribution $dF/p_t dp_t d\Delta\eta d\Delta\phi$, relative to the trigger particle angles, depends on \mathbf{q} and the initial parton momentum distribution. The momentum kick \mathbf{q} is expected to lie within a narrow cone in the trigger particle direction. To minimize the number of parameters, we approximate \mathbf{q} to lie along the trigger particle direction.

The experimental pp near-side jet data, shown as open circles in Figs. 1 and 2, can be described well by the dash-dot curves in these figures obtained from

$$\frac{dN_{\text{jet}}^{pp}}{p_t dp_t d\Delta\eta d\Delta\phi} = N_{\text{jet}} \frac{\exp\{(m - \sqrt{m^2 + p_t^2})/T_{\text{jet}}\}}{T_{\text{jet}}(m + T_{\text{jet}})} \times \frac{1}{2\pi\sigma_\phi^2} e^{-[(\Delta\phi)^2 + (\Delta\eta)^2]/2\sigma_\phi^2}, \quad (10)$$

where $\sigma_\phi = \sigma_{\phi 0} m_a / \sqrt{m_a^2 + p_t^2}$, $\sigma_{\phi 0} = 0.5$, $m_a = 1.1$ GeV, $N_{\text{jet}} = 0.75$, $m = m_\pi$, and $T_{\text{jet}} = 0.55$ GeV.

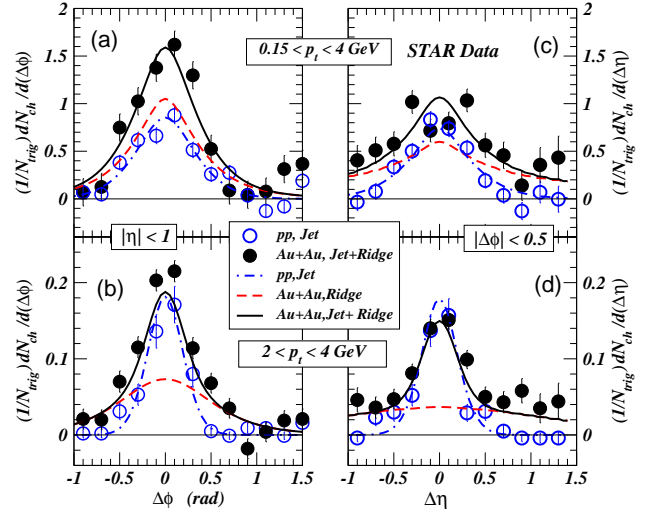


FIG. 1: The symbols represent experimental data [1] and the curves theoretical results, for pp and central AuAu collisions. (a) and (b) give the $dN_{\text{ch}}/N_{\text{trig}} d\Delta\phi$ distributions. (c) and (d) give the $dN_{\text{ch}}/N_{\text{trig}} d\Delta\eta$ distributions.

The initial momentum distribution $dF/d\mathbf{p}_i$ of the medium partons in Eq. (9) is not yet a quantity that can be obtained from first principles of QCD or the end-point, last-stage bulk data. It can however be extracted directly from the near-side ridge data. It was parametrized previously as $e^{-y_i^2/2\sigma_y^2} \exp\{-\sqrt{m^2 + p_{ti}^2}/T\}/\sqrt{m^2 + p_{ti}^2}$, with m taken to be m_π [11]. Although this is adequate for mid-rapidity and high p_t ridge particles [11], it leads to too large a ridge yield both at $p_t \sim 1$ GeV (dotted curve in Fig. 2) and at forward rapidities. If the partons arise

from a deconfined medium with a finite transverse boundary, then the transverse parton momentum distribution at small p_t will be flattened from an exponential distribution, as shown in Figs. 1 and 2 of [20]. Transverse distributions of this type can be described by replacing the denominator $\sqrt{m^2 + p_{ti}^2}$ with $\sqrt{m_d^2 + p_{ti}^2}$ where m_d can be adjusted to lead to the correct ridge yield at $p_t \sim 1$ GeV. The extracted transverse momentum distribution may provide useful information to study the transverse radius of the deconfined parton medium [20]. The difficulty with the forward rapidity region can be resolved by noting that the Gaussian rapidity distribution of [11] does not take into account the kinematic boundary restrictions on phase space. We can use a rapidity distribution that retains the flatness at mid-rapidity but also respects the kinematic boundaries at large rapidities and large p_t . Accordingly, we parametrize the normalized initial parton momentum distribution as

$$\frac{dF}{p_{ti} dp_{ti} dy_i d\phi_i} = A_{\text{ridge}} (1-x)^a \frac{e^{-\sqrt{m^2 + p_{ti}^2}/T}}{\sqrt{m_d^2 + p_{ti}^2}}, \quad (11)$$

where A_{ridge} is a normalization constant defined by $\int d\mathbf{p}_i dF/d\mathbf{p}_i = 1$, x is the light-cone variable [19]

$$x = \frac{\sqrt{m^2 + p_{ti}^2}}{m_b} e^{|y_i| - y_b}, \quad (12)$$

a is the fall-off parameter that specifies the rate of decrease of the distribution as x approaches unity, y_b is the beam parton rapidity, m_b is the mass of the beam parton whose collision and separation lead to the inside-outside cascade production of particles [19, 21, 22]. As $x \leq 1$, there is a kinematic boundary that is a function of y_i and p_{ti} ,

$$\sqrt{m^2 + p_{ti}^2} = m_b e^{y_b - |y_i|}. \quad (13)$$

We expect y_b to have a distribution centered around the nucleon rapidity, $y_N = \cosh^{-1}(\sqrt{s_{NN}}/2m_N)$. For lack of a definitive determination, we shall set y_b equal to y_N and m_b equal to m , pending their future experimental determination by examining the ridge boundaries.

We find that the totality of the STAR near-side associated particle data [1, 3, 4], in the region of $0.15 < p_t < 4$ GeV and $0 < |\eta| < 3.9$ in central AuAu collisions at $\sqrt{s_{NN}} = 200$ GeV, can be described by $|\mathbf{q}| = 1.0$ GeV, $f_R \langle N \rangle = 4$, $a = 0.5$, $T = 0.50$ GeV, and $m_d = 1$ GeV.

We shall discuss the comparison of the experimental data with theoretical results. In Figs. 1, 2, and 3, the experimental total associated particle yields [1, 4] are represented by solid circles and the theoretical total and ridge yields by solid and dashed curves, respectively. In Fig. 1, comparison of theoretical and experimental associated particle data indicates general agreement over all azimuthal angles [Figs. 1(a) and 1(b)] and over all pseudorapidities [Figs. 1(c) and 1(d)], for both $0.15 < p_t < 4$ GeV [Figs. 1(a) and 1(c)] and $2 < p_t < 4$ GeV [Figs. 2(b)

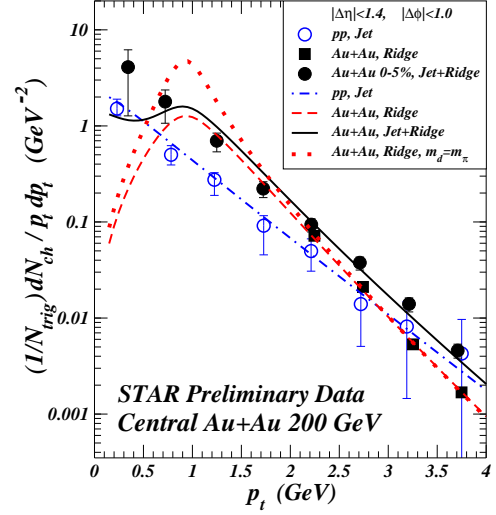


FIG. 2: The symbols represent STAR experimental data [1, 3] and the curves theoretical results of $dN_{\text{ch}}/N_{\text{trig}} p_t dp_t$, for pp and central AuAu collisions.

and 2(d)]. In Fig. 2, experimental ridge $dN_{\text{ch}}/N_{\text{trig}} p_t dp_t$ data [3] are shown as solid squares and they are calibrated by using the data of Fig. 2 of [3]. Fig. 2 shows good agreement between theoretical $dN_{\text{ch}}/N_{\text{trig}} p_t dp_t$ results with experimental data. Note that the theoretical ridge $dN_{\text{ch}}/N_{\text{trig}} p_t dp_t$ has a peak at $p_t \sim |\mathbf{q}| \sim 1$ GeV, as a result of the momentum kick.

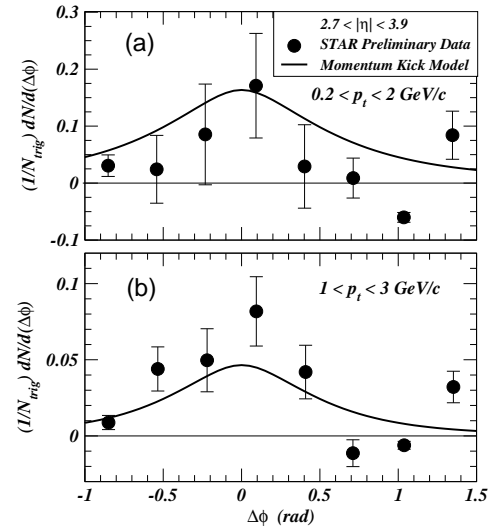


FIG. 3: STAR central AuAu collision azimuthal angle distribution data at forward pseudorapidities [4] compared with results in the momentum kick model (solid curves). (a) is for $0.20 < p_t < 2$ GeV, and (b) is for $1 < p_t < 3$ GeV.

We turn now to forward rapidities where preliminary experimental data have been obtained for $2.7 < |\eta| < 3.9$ [4]. We note that $dN_{\text{ch}}/N_{\text{trig}} d\Delta\phi d\Delta\eta$ at $\Delta\phi \sim 0$ for $|\eta| < 1$ in Fig. 1(a) is an order of magnitude greater than the corresponding $dN_{\text{ch}}/N_{\text{trig}} d\Delta\phi d\Delta\eta$ for $2.7 < |\eta| < 3.9$ in

Fig. 3(a). This implies a substantial fall-off of ridge yield $dN_{\text{ch}}/N_{\text{trig}}\Delta\phi d\Delta\eta$ at $\Delta\phi \sim 0$ in going from mid-rapidities to large rapidities. Measurements at forward rapidities in Fig. 3 contain events with large η and p_t that are either already outside the kinematic limits or close to the kinematic limits. Therefore, even with the large errors, the forward rapidity data in Fig. 3 are sensitive to the constraint of the kinematic limits and the rate of fall-off of the initial parton momentum distribution as specified by the fall-off parameter a .

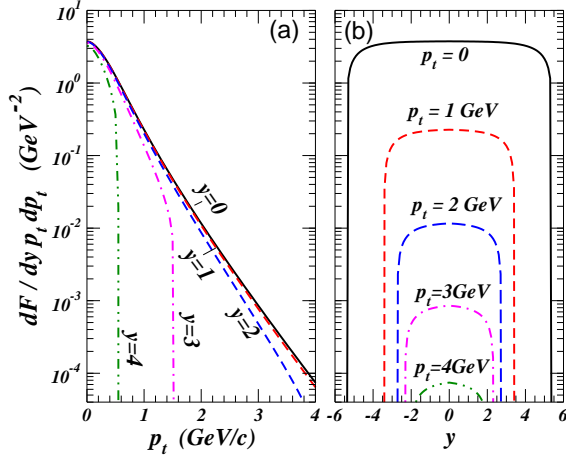


FIG. 4: Normalized initial parton momentum distribution $dF/dyp_t dp_t$ extracted from the STAR Collaboration data [1, 3, 4]. (a) $dF/dyp_t dp_t$ as a function of p_t for different y , and (b) $dF/dyp_t dp_t$ as a function of y for different p_t .

The distribution (11) with $a = 0.5$, $T = 0.50$ GeV, and $m_d = 1$ GeV gives the extracted normalized initial parton momentum distribution at the moment of jet-parton collision. We show this distribution $dF/p_t dp_t dy$ in Figs. 4(a)

and 4(b), where p_t and y are initial parton momentum variables. In Fig. 4(b), the momentum distribution as a function of y for a fixed p_t is essentially flat near central rapidities and it extends to a maximum value of $|y|_{\text{max}}$ that depends on p_t . The distribution decreases rapidly as it approaches the kinematic limit. The rapidity plateau structure suggests the inside-outside cascade picture of parton production, as in the rapidity distribution of radiated particles when a pair of color charges recede from each other [19, 21, 22].

In conclusion, the near-side ridge data in high-energy heavy-ion collisions can be explained by the picture that a jet occurs near the surface, kicks medium partons, loses energy, and fragments into the trigger particle and other fragmentation products. The kicked medium partons materialize as ridge particles which carries information on the early parton momentum distribution. The extracted early parton momentum distribution has a thermal-like transverse distribution but a rapidity plateau structure whose width decreases as the transverse momentum increases. The early parton momentum distribution provides valuable information for the mechanism of early parton production and the later evolution of the system toward the state of quark-gluon plasma.

After the manuscript was completed, predictions based on the present momentum kick model for particle yields up to large $|\Delta\eta|$ associated with a near-side jet were found to agree well with experimental measurements obtained by the PHOBOS Collaboration [23].

The author wishes to thank Profs. Fuqiang Wang, J. Putschke, V. Cianciolo, Zhangbu Xu, Jiangyong Jia, and C. Nattrass for helpful discussions and communications. This research was supported in part by the Division of Nuclear Physics, U.S. DOE, under Contract No. DE-AC05-00OR22725, managed by UT-Battelle, LLC.

-
- [1] Adams J *et al.* (STAR Collaboration) 2005 Phys. Rev. Lett. **95**, 152301
 - [2] Adams J. *et al.* (STAR Collaboration) 2006 Phys. Rev. C **73**, 064907
 - [3] Putschke J (STAR Collaboration) 2007 J. Phys. G **34**, S679
 - [4] Wang F (STAR Collaboration) 2007 [arXiv:0707.0815]
 - [5] Bielcikova J (STAR Collaboration) 2007 J. Phys. G **G74**, S929; Molnar L. (STAR Collaboration), J. Phys. G **74**, S592; Abelev B. (STAR Collaboration) 2007 [arXiv:0705.3371]
 - [6] Hwa R C and Yang B C 2003 Phys. Rev. C **67** 034902; Hwa R C and Tan Z G 2005 Phys. Rev. C **72**, 057902; Chiu C B and Hwa R C 2005 Phys. Rev. C **72**, 034903
 - [7] Hwa R C 2007 [arXiv:0708.1508]
 - [8] Romatschke P 2007 Phys. Rev. C **75**, 014901
 - [9] Voloshin S A 2005 Nucl. Phys. A **749**, 287
 - [10] Armesto A, Salgado C A, Wiedemann U A 2004 Phys. Rev. Lett. **93**, 242301
 - [11] Wong C Y 2007 Phys. Rev. C **76**, 054908
 - [12] Wong C Y 2008 J. Phys. G **35**, 104085 [arXiv:0804.4017]
 - [13] Wong C Y 2008 [arXiv:0806.2154]
 - [14] Shuryak E 2007 Phys. Rev. C **76**, 047901.
 - [15] Pantuev V S 2007 [arXiv:0710.1882]
 - [16] Dumitru A, Nara Y, Schenke Y B, and Strickland M 2007 [arXiv:0710.1223].
 - [17] S. Gavin, and G. Moschelli, J. Phys. G **35**, 104084 (2008).
 - [18] A. Dumitru, F. Gelis, L. McLerran, and R. Venugopalan, [arXiv:0804.3858].
 - [19] Wong C Y *Introduction to High-Energy Heavy-Ion Collisions*, World Scientific Publisher, 1994
 - [20] Mostafa M and Wong C Y 1995 Phys. Rev. C **51**, 2135
 - [21] Casher A, Kogut J, and Susskind L 1974 Phys. Rev. D **10**, 732.
 - [22] Wong C Y, Wang R C and Shih C C 1991 Phys. Rev. D **44**, 257
 - [23] Wenger E (PHOBOS Collaboration) 2008 J. Phys. G **35**, 104080 [arXiv:0804.3038]